Int J Adv Manuf Technol (2017) 92:1411–1424
DOI 10.1007/s00170-017-0201-9

ORIGINAL ARTICLE

Analysis of the machine tool dynamic characteristics in manufacturing space based on the generalized dynamic response model

Congying Deng[1] · **Yun Liu**[2] · **Jie Zhao**[1] · **Bo Wei**[1] · **Guofu Yin**[2]

Received: 2 October 2016 / Accepted: 22 February 2017 / Published online: 11 March 2017

Abstract Machine tool dynamic characteristics are seriously affected by the changes of the machining poses and the spindle bearing joints dynamic properties. As these changes contribute much more complexity and uncertainty for predicting the machine tool dynamic characteristics accurately, a new method is developed to research the changing regularity of the whole machine tool dynamic characteristics in generalized manufacturing space. In this method, the dynamic flexibilities at the spindle nose of *x*, *y,* and *z* directions in the focused frequency range are taken to represent the whole machine tool dynamic characteristics. The response surface method (RSM) and the orthogonal experiment design method are combined to establish the generalized dynamic response model, which contains the information of the spatial poses and the spindle bearing dynamic parameters. To establish this model, the simulations arranged by the orthogonal design are conducted by utilizing the dynamic model modified approach based on the validated finite element model (FEM) of the whole machine tool. With evaluating the fitting degree of this generalized dynamic response model, it can be used to predict the dynamic characteristics in the manufacturing space. Furthermore, an algorithm based on the established model is proposed to calculate the effect factors acting on the whole machine tool dynamic characteristics, which are caused by the changes of the spindle bearing dynamic parameters. The proposed analytical method has been applied in a three-axis vertical machining center to establish its generalized dynamic response model. The dynamic flexibilities at the spindle nose in the generalized manufacturing space are predicted, and they are validated by the dynamic experiments. With the calibrated model, effect factors of the spindle bearing joints are also obtained. All the predicted results support a theoretical basis on the optimal process routes planning, and the proposed analytical method can lay a foundation for further study on the dynamic information of the tool point.

Keywords Machine tool dynamics · Generalized manufacturing space · Joint dynamic properties · Response surface method

✉ Congying Deng
dengcy@cqupt.edu.cn

[1] School of Advanced Manufacturing Engineering, Chongqing University of Posts and Telecommunications, Chongqing 400065, China

[2] School of Manufacture Science and Engineering, Sichuan University, Chengdu 610065, China

1 Introduction

Machine tool dynamic characteristics have a great influence on the machining quality and machining efficiency, which include natural frequency, dynamic stiffness, dynamic flexibility, modal shapes, etc. In order to investigate the whole machine tool dynamic characteristics accurately, methods to build the machine tool dynamic model, obtain these dynamic parameters and conduct the optimization have been examined in detail for decades [1–4].

Park et al. [5] put forward an enhanced receptance coupling methodology by utilizing the comparative study on experimental and finite-element (FE) analyses to identify the joint dynamics between substructures, with which dynamic properties of the modular tools had been predicted, enabling designers to optimize the dynamic behavior in the conceptual stage. Hung et al. [6] constructed an accurate finite element model of the vertical spindle tooling system to research the interactive influence of the spindle unit and the machine frame

structure on the machining stability, in which the bearing stiffness of the rolling elements within ball bearings, ball screw, and linear guides were taken into consideration. Kolar et al. [7] created a coupled model of the whole mechanical system, in which the spindle detailed model and machine frame FE model were jointed. Shift in the spindle and tool system dynamic properties, related to the machine frame properties, is proved by utilizing this coupled model.

With these methods and models, designers can analytically evaluate and then optimize the whole machine tool dynamic characteristics at the design stage [8–11]. Nevertheless, when designing and analyzing the whole machine tool dynamic characteristics, these approaches are usually confined to a specific machine tool pose. Thus, the obtained dynamic parameters cannot accurately describe the whole machine tool dynamic characteristics in manufacturing space. By means of the virtual environment simulations and the dynamic experiments, methods to evaluate the dynamic characteristics of the whole machine tool which depend on the poses of the moving parts have been proposed [12, 13].

Liu et al. [14] have defined the generalized manufacturing space functions to conduct the modal and response analyses. The obvious modal frequency change rate illuminated the importance to obtain the complete modal information in manufacturing space. Sun et al. [15] identified how the distributed joint dynamic parameters affected the machine tool dynamic stiffness at the spindle nose in generalized manufacturing space, which provided a technique support for the quantitative design of joints dynamic parameters.

For machining process, the changes of the machining poses and the spindle bearing dynamic parameters are working together on the machine tool dynamic characteristics. However, researches on the change tendency and the correlation of the whole machine tool dynamic performance with different machining poses, and spindle bearing dynamic properties are relatively few [16–19].

In this study, an analytical method to predict the machine tool dynamic characteristics in the generalized manufacturing space is proposed. In the method, a generalized dynamic response model that considers the information of the machining poses and the spindle bearing dynamic properties is established. This model is based on the response surface method and the orthogonal experiment method, in which the accurate whole machine tool FEM is the prerequisite, and the dynamic model modified method is adopted to realize the simulations arranged by the orthogonal experiment design. With the established generalized dynamic response model, variations of the generalized dynamic flexibilities at the spindle nose can be investigated. An algorithm is developed to calculate the effect factors causing by the changes of the spindle bearing dynamic parameters, which act on the whole machine tool dynamic flexibilities in the manufacturing space. The proposed method is applied in a three-axis vertical machining center, and its feasibility is verified by the dynamic experiments. With the calibrated analytical model, the variations of the dynamic flexibility at the spindle nose in the case of multi-axis linkage are studied. Also, the effect factors caused by the changes of the axial and radial spindle bearing dynamic stiffness are calculated to research their influencing degree on the dynamic flexibilities in the generalized manufacturing space. Those results provide an approach on the optimal machining pose choice and process routes planning.

2 Spatial dynamic characteristics of whole machine tool

In the machine tool dynamics theory, dynamic equation of the machine tool considering the joints properties can be determined as follows:

$$\mathbf{m}\ddot{\mathbf{x}}+\left(\mathbf{c}+\mathbf{c_j}\right)\dot{\mathbf{x}}+\left(\mathbf{k}+\mathbf{k_j}\right)\mathbf{x}=\mathbf{f} \tag{1}$$

In the above equation, $\boldsymbol{m}$ is the mass matrix of machine tool. $\boldsymbol{c}$ and $\boldsymbol{k}$ are the damping matrix and the stiffness matrix of the machine tool substructure, respectively. $\boldsymbol{c_j}$ and $\boldsymbol{k_j}$ are the damping matrix and the stiffness matrix of the joints, respectively. $\boldsymbol{f}$ is the total external force matrix.

Referring to the modal theory for vibration characteristics, the dynamic flexibility $W_{ba}(\omega)$ between the excitation point A, and the response point B can be described as Eq. (2):

$$W_{ba}(\omega)=\frac{X_b}{F_a}=\sum_{r=1}^{\infty}\frac{1}{\left[1-\left(\frac{\omega}{\omega_r}\right)^2+i2\xi_r\left(\frac{\omega}{\omega_r}\right)\right]}\left(\frac{A_a{}^{(r)}A_b{}^{(r)}}{K_r}\right) \tag{2}$$

Where $A_a{}^{(r)}$ and $A_b{}^{(r)}$ are the r_{th} relative displacement amplitude of point A and point B, respectively; K_r is the r_{th} dynamic modal stiffness; ω_{nr} is the r_{th} natural frequency; ζ_{nr} is the r_{th} modal damping.

In the machining process, the mass matrix, stiffness matrix , and damping matrix are varying as the pose changes of the components, which means that these matrixes and the whole machine tool dynamic characteristics related to them are functions of the linear and angular displacements [20–22]. The whole machine tool dynamic characteristics largely depend on the dynamic properties of the spindle system, and the spindle system properties are always characterized by the tool point frequency responses (FRFs), which are also important for the machining stability identification [23, 24]. The clamping holder-tool system is varied for different machining objects and processes, which causes many difficulties and uncertainties to predict the dynamic information of the tool point at each machining condition. As the dynamic information at the spindle nose accounts for much of the whole machine tool dynamics and its weak parts greatly affect the tool dynamic information, for simplicity, without taking the

mounted tool system into consideration, the dynamic flexibility $W_{ba}(\omega)$ at the spindle nose is utilized as an important index to evaluate the dynamic characteristics of the machine tool. Furthermore, to study how the changes of the spindle bearing dynamic parameters affect the whole machine tool dynamic characteristics, function for the dynamic flexibility can be defined as follows:

$$W_G(\omega) = F\left(x, y, z, \theta_i, k_j\right) \tag{3}$$

Where x, y and z are the axial displacements of their corresponding directions; θ_i is the angular displacements of the rotation axes; k_j stands for the spindle bearing joint dynamic stiffness.

The mathematical model established based on Eq. (3) contains information of the machining poses and the joint dynamic properties. It can be used to describe the changing regularity of the whole machine tool dynamic flexibility in the generalized manufacturing space.

3 Establishment of the generalized dynamic response model based on RSM

In this section, with the defined Eq. (3), a generalized dynamic response model is established to predict the machine tool dynamic characteristics based on the RSM method and the orthogonal experiment method.

3.1 The RSM theory

RSM utilizes the experiment design theory to conduct experiments with the chosen sample points, and then construct the approximate model to describe the relationships among the objectives, constraints, and designed variables [25]. Then the responses related to the non-experiment sample points can be predicted. Generally, the relationships can be approximated by a low order polynomial in a region of the independent variables. For the complicated system, the quadratic polynomial is usually adopted. When n experiments have been designed, the quadratic polynomial of the RSM can be expressed as Eq. (4):

$$\begin{aligned} \mathbf{Y} &= \hat{\mathbf{Y}} + \boldsymbol{\varepsilon} \\ \hat{\mathbf{Y}} &= \mathbf{X}\boldsymbol{\beta} \end{aligned} \tag{4}$$

Where $\boldsymbol{Y}$ is the response vector; $\hat{\mathbf{Y}}$ is the estimated response vector; X is the matrix of the design variables; $\boldsymbol{\beta}$ is the regression coefficients vector; $\boldsymbol{\varepsilon}$ is the random error vector. To minimize the $\boldsymbol{\varepsilon}$, the least squares are employed to find a response surface closing to all experiment data:

$$Min \rightarrow S(\beta) = \sum_{i=0}^{m-1}\left(\varepsilon^2\right) = \sum_{i=0}^{m-1}(Y - X\beta)^2 \tag{5}$$

The requisite to obtain the minimum values of Eq. (5) is as follows:

$$\frac{\partial S}{\partial \beta} = 2\sum_{i=0}^{m-1}\left[x^{(i)}\left(\sum_{j=0}^{p-1}\left(\beta_i x_j^{(i)} - y^{(i)}\right)\right)\right] \tag{6}$$

$$(X\beta - Y)^{\mathrm{T}} X = 0 \tag{7}$$

$$\beta = \left(X^{\mathrm{T}}X\right)^{-1}X^{\mathrm{T}}Y \tag{8}$$

Appling Eq. (8) into Eq. (4), the mathematical expressions for the response surface function can be obtained. To validate the accuracy of the established approximate model, the relative value of root mean square error (RMSE) and the coefficients of determination R^2 are adopted to evaluate its fitting degree of the samples [17].

$$\left.\begin{aligned} R_{mse} &= \frac{1}{m\overline{w}}\sqrt{\sum_{i=1}^{m}\left(w_i - \tilde{w}_i\right)^2} \\ R^2 &= 1 - \frac{\sum_{i=1}^{m}\left(w_i - \tilde{w}_i\right)^2}{\sum_{i=1}^{m}\left(w_i - \overline{w}_i\right)^2} \end{aligned}\right\} \tag{9}$$

Where m is the number of the sample points; w_i and $\overline{w}$ is the results calculated through the FE analysis and their average values respectively, and $\tilde{w}_i$ is the results predicted by the approximate model. If RMSE trends to 0, it means less error. If R^2 trends to 1, it means a higher fitting degree.

3.2 The generalized dynamic response model

According to the RSM theory, approaches to establish the generalized dynamic response model is illustrated as follow:

1. The objective functions, design variables and constraints

$$\begin{aligned} &\text{objective}(\mathbf{w_d}) \\ &\text{s.t.} \quad x_{\min} \le x \le x_{\max} \\ &\qquad y_{\min} \le y \le y_{\max} \\ &\qquad z_{\min} \le z \le z_{\max} \\ &\qquad \theta_{\min} \le \theta \le \theta_{\max} \\ &\qquad k_{\min} \le k \le k_{\max} \end{aligned} \tag{10}$$

In Eq. (10), the dynamic flexibilities at the spindle nose are the objectives, the linear and angular displacements and the joints dynamic parameters are the design variables, and the constraints are the travel limitation of each linear and rotational axis.

For the dynamic flexibilities varies as the changes of the frequency, it is impossible to establish the generalized dynamic response model for each specific dynamic flexibility value

at its corresponding frequency. Thus, to have a more comprehensive understanding on the whole machine tool characteristics, it needs to carry the segmentation on the focused frequency range, and the maximum dynamic flexibility at each segment along its related direction is regarded as the objective to characterize the worst resistance ability of the forced vibration. Then, the objectives of Eq. (10) are expanded as Eq. (11):

$$\mathbf{w_d} = \begin{bmatrix} w_{dx\omega_1} & w_{dx\omega_2} & \cdots & w_{dx\omega_n} \\ w_{dy\omega_1} & w_{dy\omega_2} & \cdots & w_{dy\omega_n} \\ w_{dz\omega_1} & w_{dz\omega_2} & \cdots & w_{dz\omega_n} \end{bmatrix} \tag{11}$$

Where the subscripts x, y, and z mean the directions; the subscripts ω_1, $\omega_2 \ldots$, ω_n stand for the segments of the focused frequency range.

2. The orthogonal experiment design

As the sample points have different values, it is difficult and a waste of time to study the whole machine tool dynamic characteristics corresponding to all the combinations of each value belonging to the variables. Then, the orthogonal experiment design method is introduced to arrange the experimental schemes to obtain the results of the whole machine tool dynamic characteristics within the given sample points [26]. The orthogonal experiment design method is based on the orthogonality to select the representative points from the comprehensive experiment, which is usually adopted to fulfill the multifactor and multilevel experiment.

People have tabulated the level selection for each factor. Thus, when using the orthogonal experiment design method, the appropriate orthogonal table should be chosen according the number of the factors and levels. For instance, if there are three factors and each one has four levels, then the orthogonal table $L_9(3^4)$ can be chosen, in which nine experiments are arranged to execute. These experimental results are regarded as the data input to the response surface method.

3. The generalized dynamic response model

To establish the generalized model, it needs to obtain the dynamic flexibilities at the spindle nose in three directions with the specific sample space according to the orthogonal experiment design. To build the dynamic model of the whole machine tool with different poses and spindle bearing dynamic parameters, the finite element model (FEM) of the whole machine tool structure is established in the virtual simulation environment. For establishing the accurate whole machine tool FEM, the dynamic parameters of the key joints distributing in the whole machine tool structure should be identified. And the dynamic model modified method is applied for rebuilding the whole machine tool FEM. In this research, the whole machine tool FEM of each designed discrete space pose is rebuilt by controlling the joint nodes, and they are connected by the spring-damper elements with the identified joints dynamic parameters. Accordingly, utilizing the ANSYS software to build the FEM of the whole machine tool and conduct the dynamic analyses, the major procedures to establish the generalized dynamic response model can be summarized as below:

a. Choose the appropriate orthogonal table to design the sampling experiments with the given values of the variables.
b. Manually mesh the simplified three dimensional geometric models of the components to build their FEMs, and the joint nodes at their contact surfaces are defined. These node numbers are recorded to add the spring-damper elements after their spatial coordinates are determined.
c. Reassemble the FEM of these components with the specific spatial coordinates of the joint nodes and their related joints dynamic parameters according to the orthogonal table. Then, the updated FEM can represent the dynamic model of the whole machine tool with the varying poses and spindle bearing joints dynamic parameters in the generalized manufacturing space.
d. Compile multiple analysis files with the parameterized languages (APDL) offered by the ANSYS software in order to create the sample space of the whole machine tool FEM. The recorded joint node numbers and their related dynamic stiffness and damping coefficients are written in these files to add the spring-damper elements at the designed positions.
e. Adopt these updated FEMs to conduct the modal and harmonic analyses. Thus, the maximum dynamic flexibilities in three directions for each segment of the focused frequency range are obtained and saved as files.
f. With the simulated results, the generalized dynamic response model is established by referring to the previously mentioned formulas from (4) to (11).

4. The effect factors of the spindle bearing joints dynamic parameters

Usually, the axial and radial dynamic stiffness and damping are identified to simulate the dynamic properties of the spindle bearing joints. As the damping mechanism is too complicated too research into deeply and the accurate damping is difficult to obtain, the effects of the dynamic stiffness that varies as the changes of the spindle speed are firstly discussed. To study how the changes of the axial and radial stiffness affect the dynamic flexibilities at the spindle nose in the corresponding directions and frequency segments, an algorithm to calculate the effect factors is proposed.

In the machining process, the dynamic stiffness of the spindle bearing joints intenerates with the rising rotating speed

owing to the centrifugal force. Thus, assuming that a unit value change has happened to the obtained dynamic stiffness of the spindle bearing joints, the updated dynamic stiffness can be represented as Eq. (12):

$$\begin{aligned} k_{ai}{}' &= k_{ai} - \Delta k \\ k_{ri}{}' &= k_{ri} - \Delta k \end{aligned} \tag{12}$$

Then, the effect factor is defined as the weight, which stands the change of the dynamic flexibility caused by the decrease of the bearing dynamic stiffness that accounts for the original dynamic flexibility. It represents an index to evaluate the influential degree of the decreasing dynamic stiffness of the spindle bearings on the generalized whole machine tool dynamic characteristics.

Taking the updated dynamic stiffness as the input of the established generalized dynamic response model to predict the related dynamic flexibilities, the effect factors in the generalized manufacturing space are calculated through Eq. (13). Then, according to the matrix form of Eq. (11), the same decomposition for the directions and frequency segments are carried out on the effect factors:

$$\begin{aligned} E_{k_i} &= \frac{\Delta w\left(k_{ai}{}', k_{ri}{}'\right)}{w(k_1, k_2, \cdots, k_n)} \Delta w\left(k_{ai}{}', k_{ri}{}'\right) \\ &= w\left(k_1, k_2, \cdots, k_{ai}{}', k_{ri}{}' \cdots, k_n\right) - w(k_1, k_2, \cdots, k_n) \end{aligned} \tag{13}$$

$$\mathbf{E} = \begin{bmatrix} E_{x\omega_1} & E_{x\omega_2} & \cdots & E_{x\omega_n} \\ E_{y\omega_1} & E_{y\omega_2} & \cdots & E_{y\omega_n} \\ E_{z\omega_1} & E_{z\omega_2} & \cdots & E_{z\omega_n} \end{bmatrix} \tag{14}$$

4 Case study on a vertical machining center

The proposed method to study the generalized dynamic characteristics of a whole machine tool has been applied in a three-axis vertical machining center, and the application procedure is described as Fig. 1.

Figure 2 is the studied whole vertical machining center, which is mainly assembled with the bed, the column, the saddle, the worktable, the headstock, the spindle, and the typical joints. In the three-axis vertical machining center, the worktable, saddle, and headstock travel in the x, y, and z direction respectively, which are driven by the linear guides and ball screws.

4.1 The FEM of the whole vertical machining center

According to researches, there are four types of joints in the vertical machining center, in which the linear guide, bolt joint, bearing, and ball screw are included [27, 28]. To establish the accurate FEM of the whole machine tool structure, the dynamic properties of these typical joints should be identified. As the approaches to identify the dynamic parameters of these joints and validate the accuracy of the whole machine tool FEM have been concretely discussed earlier by the authors in Ref. [29], only the brief procedures and results of these identifications are described in this paper.

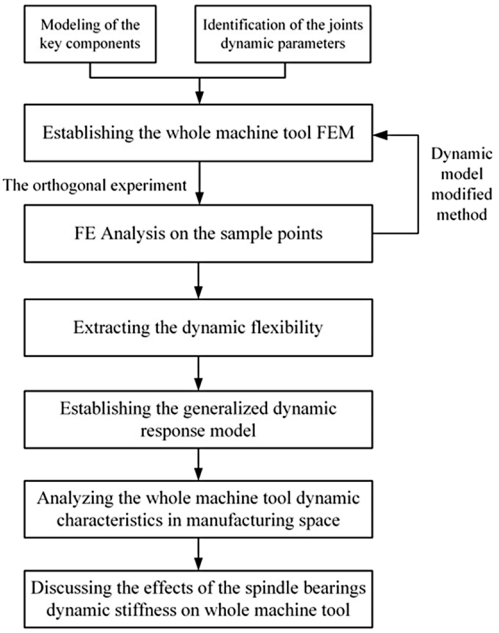

Fig. 1 The application procedure

1. The linear guide joint

The identification combines the FE analysis and the modal experiment, in which the dynamic stiffness and damping of

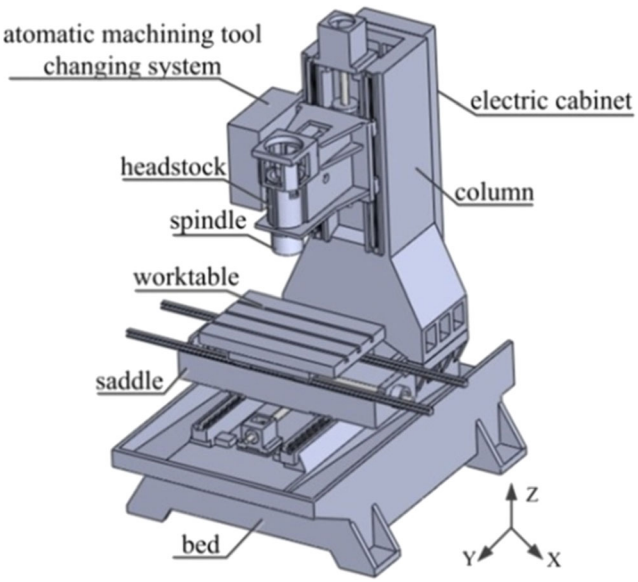

Fig. 2 The studied vertical machining center

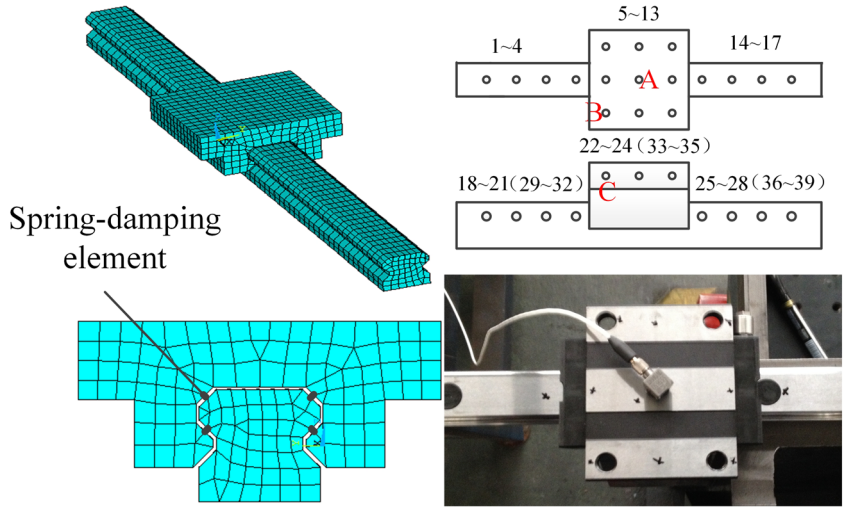

Fig. 3 The dynamic model and experiment of the joint

the linear guide are obtained based on the optimal algorithm. If the natural frequency and damping ratio errors between the modal experiment and the simulation are acceptable, the stiffness and damping coefficients estimated in the simulation can be regarded as the dynamic stiffness and damping coefficients of the linear guide. Figure 3 depicts the dynamic model of the linear guide, and its identified dynamic stiffness and damping coefficients are 6.07×10^8 N/m and 5280 N•s/m.

2. The bolt joint

The contact pressure of one bolt joint is described as Eq. (15).

$$P_n = \frac{2T}{\left[D_1 \tan(\rho_v + \beta_b) + 2\mu_c \frac{\left(D_2{}^3 - D_1{}^3\right)}{3\left(D_2{}^2 - D_1{}^2\right)}\right] AN} \tag{15}$$

Where T is the tightening torque, A is the area of the bolt joint, and N is the number of bolts. The other parameters in Eq. (15) can be calculated by referring to the third section of the Ref. [29].

Researches have presented the contact stiffness and damping under different pressure. With the pressure calculated by Eq. (15), the contact stiffness and damping under the same contact conditions are obtained by consulting these researches. Taking the key bed-column bolt joint as an instance, its rough degree is 1.6 and the pressure is 6.4Mpa. The obtained dynamic stiffness and damping from Ref. [30] and Ref. [31] are listed in Table 1, and the bolt joint dynamic model is depicted in Fig. 4.

Table 1 The parameters of the bolt joints

Direction	Stiffness(N/m)	Damping(N·s/m)
Normal	4.63×10^{10}	6.9×10^9
Tangential	1.08×10^6	1.12×10^5

3. The bearing joint

The inner ring and outer ring of the bearing are connected by the elastic spring elements as shown in Fig. 5. The contact stiffness is obtained from the product selection guide, which is listed in Table 2. To avoid the complexity for creating and meshing the 3D model of the bearing, the balls and ball grove are ignored.

4. The ball screw joint

The ball screw studied in this paper is used to carry the major load in the feeding direction. The axial and radial stiffness of the ball screw is determined based on the properties of the screw and nut and their geometrical relationships. Its simplified 3D and FE models are shown in Fig. 6, in which the helical groove around the screw shaft and the nut are ignored. The axial stiffness between the nut and screw is simulated by the spring element between the nut and load. The contact stiffness obtained from the manufacturer is listed in Table 3.

5. FEM of the whole machine tool

With the FEM of the key components and the identified joint parameters, the FEM of the whole machine tool is established as shown in Fig. 7. To validate its accuracy, the simulation and the experiment are conducted, and their boundary conditions should be consistent. Then, the simulated and

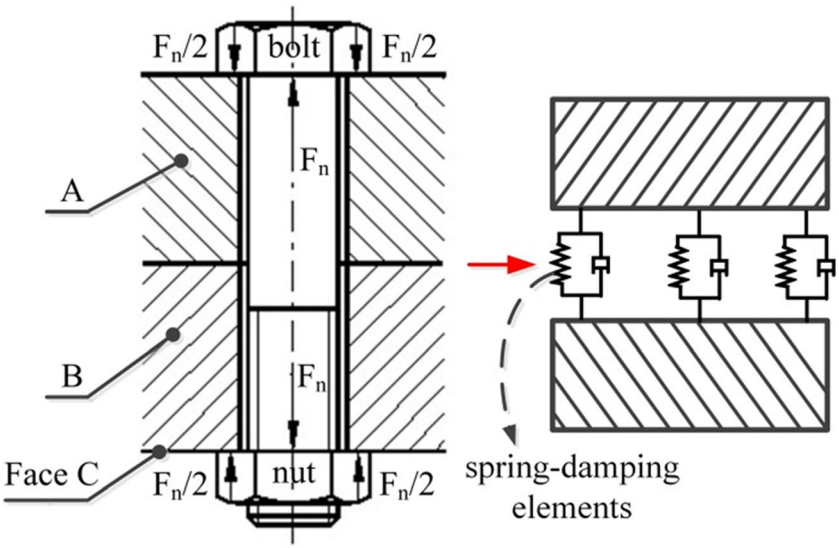

Fig. 4 The bed-column bolt joint dynamic model

experimental modal frequencies and frequency response functions (FRFs) at the spindle nose in three directions are compared to demonstrate the accuracy of the established FEM.

4.2 The generalized dynamic response model of the vertical machining center

To predict the dynamic characteristics of the whole vertical machining center in the generalized manufacturing space, its generalized dynamic response model are built in this section.

1. Construction of the response surface model

As the vertical machining center is only a three-axis machine tool and its front and rear spindle bearings are the same, a quadratic polynomial with five design variables are utilized to describe the response surface approximate model as Eq. (16) expressed according to section 3.1.

$$\begin{aligned}\mathbf{w}_d(x,y,z,k_a,k_r) = {} & \beta_1 x^2 + \beta_2 y^2 + \beta_3 z^2 + \\ & \beta_4 {k_a}^2 + \beta_5 {k_r}^2 + \beta_6 x + \beta_7 y + \beta_8 z + \\ & \beta_9 k_a + \beta_{10} k_r + \beta_{11} xy + \beta_{12} xz + \beta_{13} x k_a + \\ & \beta_{14} x k_r + \beta_{15} yz + \beta_{16} y k_a + \beta_{17} y k_r + \\ & \beta_{18} z k_a + \beta_{19} z k_r + \beta_{20} k_a k_r + \beta_{21}\end{aligned} \tag{16}$$

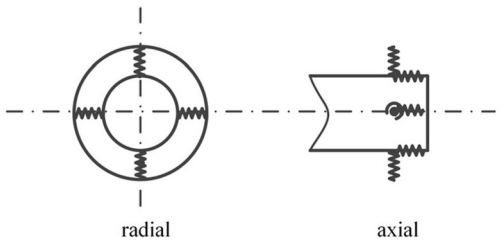

Fig. 5 The bearing joint dynamic model

Where x, y and z are the axial displacements of their corresponding directions; k_a and k_r are the axial and radial dynamic stiffness of the spindle bearing joints, respectively.

As the travel limitation of the x, y, and z directions are 0.4, 0.55, and 0.4 m, respectively, and by referring to the technique information of the spindle bearings, the factors and levels of the orthogonal experiment design are listed in Table 4. Then, the orthogonal experiment table $L_{25}(5^6)$ are chosen, in which 25 experiments are designed as shown in Table 5.

The focused frequency range of the studied vertical machining center is 0 ~ 600 Hz according to its actual manufacturing process. Thus, the total focused frequency range is divided into three parts, which are the high frequency segment (400–600), the medium frequency segment (200–400), and the low frequency segment (0–200), respectively.

Combining the orthogonal experiment design method and the dynamic model modified method, the FEM of the whole vertical machining center is modified to achieve the experiment requirements arranged by the orthogonal table. Although the joint dynamic parameters are affected by the position of the contact surface, the effects are confined by the preload and contact materials [32]. The moving linear guides and ball screws studied in this research are highly preloaded, and the contact materials are steel–steel. Furthermore, dynamic experiments have been conducted on the linear guides at three different positions along the saddle, and the identified dynamic joint parameters show little differences. Thus, for simplicity, joint dynamic parameters are assumed to be position independent [33]. Then, the maximum dynamic flexibility at the spindle nose of each frequency segment in each direction is obtained through the modal analysis and harmonic analysis in the ANSYS software. Analyzing the simulated results of the designed arrangements, it shows that the changes of these factors have hardly effects on the dynamic flexibilities in the x direction, which will cause the invalid response surface

Table 2 Basic parameters of the bearings

Type	Outer diameter D/mm	Inner diameter d/mm	Width B/mm	Contact angle β	Preload P/N	Stiffness of bearing	
						Axial/(N/m)	Radial(/N/m)
7012C(spindle bearing)	60	95	18	15	100	0.53×10^8	3.45×10^8
25TAC62B	62	25	15	60	1490	7.33×10^8	–

model. Thus, utilizing the least square method in the MATBLE software, the generalized dynamic response model is established only at the three frequency segments in y and z directions. According to Eq. (4) and Eq. (16), the quadratic polynomial is described as Eq. (17).

$$\mathbf{w} = \left[w_{dy\omega_l} \;\; w_{dy\omega_m} \;\; w_{dy\omega_h} \;\; w_{dz\omega_l} \;\; w_{dz\omega_m} \;\; w_{dz\omega_h}\right]^{\mathrm{T}} = \mathbf{X}\boldsymbol{\beta} \quad (17)$$

Where the coefficients matrix β:

$$\boldsymbol{\beta} = \begin{bmatrix}
1.36 & 0.678 & 0.572 & 0.261 & -0.214 & -0.0999 \\
0.656 & 0.754 & 0.651 & 0.453 & -0.0654 & 0.4 \\
1.11 & 0.879 & 0.668 & 0.515 & -0.186 & -0.038 \\
-1.72 & -12.1 & -9.46 & -8.16 & 0.598 & -12.1 \\
0.103 & -0.313 & -0.242 & -0.337 & -0.0739 & -0.293 \\
-6.02 & -5.01 & -3.97 & -2.5 & 0.863 & -2.03 \\
-5.51 & -5.41 & -4.51 & -2.78 & 0.736 & -2.53 \\
6.02 & 7.09 & 6.04 & 4.14 & -0.767 & 4.54 \\
9.1 & 8.82 & 3.73 & 1.81 & -1.46 & 2.24 \\
-1.2 & -0.339 & 0.369 & 0.718 & 0.249 & 0.514 \\
1.52 & 1.75 & 1.49 & 1.06 & -0.232 & 0.747 \\
-2.14 & -3.42 & -3.09 & -2.35 & 0.208 & -2.49 \\
-0.165 & 0.924 & 1.63 & 0.794 & -0.0138 & 3.03 \\
-0.0533 & 0.511 & 0.3 & 0.408 & 0.104 & 0.409 \\
-1.61 & -1.86 & -1.57 & -1.14 & 0.243 & -0.891 \\
0.113 & -0.0895 & 0.0253 & -0.112 & -0.0651 & 0.0247 \\
0.208 & 0.118 & 0.0342 & 0.00619 & -0.0386 & 0.0331 \\
-1.12 & 2.56 & -0.00187 & 2.58 & 0.48 & 4.31 \\
0.0808 & 0.034 & -0.00187 & -0.0076 & -0.0318 & -0.074 \\
-0.564 & 1.74 & 1.11 & 1.54 & 0.316 & 1.18 \\
2.13 & 1.36 & 1.52 & 1.16 & 1.97 & 7.36
\end{bmatrix}$$

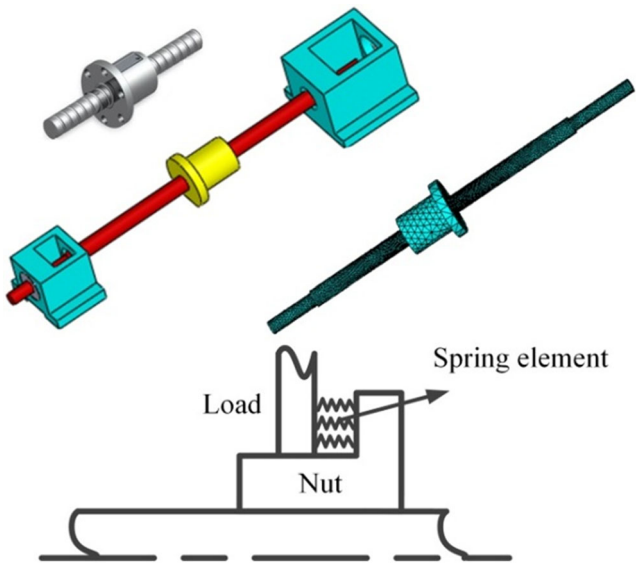

Fig. 6 The ball screw dynamic model

The unit of the dynamic flexibility in Eq. (16) is 10^{-8} m/N, and the standards to evaluate the fitting degree are calculated as listed in Table 6.

The calculated RMSE and R^2 show that the constructed generalized dynamic response model has a good fitting degree. To further study the accuracy of this model, dynamic experiments have been conducted according to the orthogonal experiment arrangements, as shown in Fig. 8. Nine machining positions were determined according to Table 7, which were not selected in the previous simulations. The comparisons of the predicted and experimental results are listed in Table 8. All the calculated and experimental results verify the feasibility of the constructed generalized dynamic response model, which can be used to predict the dynamic characteristics of the whole vertical machining center in the generalized manufacturing space.

For instance, with the given joints parameters in section 4.1 and three different locations along the y direction, Fig. 9 depicts the change regularity of the dynamic flexibilities at the spindle nose corresponding to each direction and frequency segment in the manufacturing space. As the linear guide moving along the y direction, these dynamic flexibilities at the spindle nose of the positions with the same coordinate (x,z) are different. The dynamic flexibilities of the high frequency segment in the z direction are affected less by the movement of the y directional linear guide. Thus, once this mode is probable to be the dominant mode according to the machining conditions, and the machining position can be reached by the movement of the y directional linear guide, the y directional linear guide should be driven firstly to ensure the machining stability. Studying the sub-pictures of Fig. 9a, b, c, respectively, the influences caused by the axial displacements on the dynamic flexibilities are varied for the different directions and frequency segments. The dynamic flexibilities of the medium frequency in the z direction has a smaller value, which means these corresponding positions have a relative better vibration resistance. Since the higher values of the dynamic flexibilities mean more badly responses to the vibration, the machining should be avoided to under their corresponding locations. Then, considering the specific machining conditions, Fig. 9 can guide us to work out the optimal machining pose and processing route.

Table 3 Basic parameters of the ball screw

Nominal diameter d_o/mm	Ball diameter d_b/mm	Travel P_t/mm	Contact angle β/(°)	Rows × turns	Rigidity (N/μm)
32	6.35	16	45	1 × 3.5	672

4.3 The effect factors of the spindle bearing joint dynamic parameters

Based on the established generalized dynamic response model and the algorithm for calculating the joint effect factors described as Eq. (13) and Eq. (16) respectively, the variations of the dynamic flexibilities at the spindle nose that caused by the unit change of the axial stiffness and the radial stiffness are represented as Eq. (18).

$$\begin{aligned}&\Delta w(x,y,z,k_a-\Delta k,k_r-\Delta k)\\&=\left|\begin{matrix}w(x,y,z,k_a-\Delta k,k_r-\Delta k)-\\w(k_1,k_2,z,k_a,k_r)\end{matrix}\right|\\&=\left|\begin{matrix}-(\beta_{13}+\beta_{14})x-(\beta_{16}+\beta_{17})y-\\(\beta_{18}+\beta_{19})y+\beta_4\left(-2k_a+{}^a\Delta k\right)+\\\beta_5\left(-2k_r+{}^r\Delta k\right)-\beta_{20}\left(k_r+{}^rk_a{}^a\right)-\\\beta_9-\beta_{10}+\beta_{20}\Delta k\end{matrix}\right|\times\Delta k\end{aligned}\tag{18}$$

Then, the effect factors of the axial and radial stiffness can be expressed as Eq. (19).

$$E_k=\frac{\left|\begin{matrix}-(\beta_{13}+\beta_{14})x-(\beta_{16}+\beta_{17})y-\\(\beta_{18}+\beta_{19})z+\beta_4\left(-2k_a+{}^a\Delta k\right)+\\\beta_5\left(-2k_r+{}^r\Delta k\right)-\beta_{20}\left(k_r+{}^rk_a{}^a\right)-\\\beta_9-\beta_{10}+\beta_{20}\Delta k\end{matrix}\right|\times\Delta k}{\left|\begin{matrix}\beta_1x^2+\beta_2y^2+\beta_3z^2+\beta_4{k_a}^2+\beta_5{k_r}^2+\\\beta_6x+\beta_7y+\beta_8z+\beta_9k_a+\beta_{10}k_r+\\\beta_{11}xy+\beta_{12}xz+\beta_{13}xk_a+\beta_{14}xk_r\\+\beta_{15}yz+\beta_{16}yk_a+\beta_{17}yk_r+\beta_{18}zk_a\\+\beta_{19}zk_r+\beta_{20}k_ak_r+\beta_{21}\end{matrix}\right|}\tag{19}$$

The FE simulations show that a smaller value assigned to Δk will result in unobvious effects on the dynamic flexibilities; however, the Δk with a bigger value will influence the prediction accuracy of the established approximate model. Thus, the Δk is determined to be a unit value which has the same order of magnitude as the spindle bearing joints stiffness. Substituting the identified bearing joints stiffness in Table 2 and the calculated coefficients matrix β into Eq. (19), the effect factors are the functions of the axial displacements of the x, y and z directions. It means that the variation of the machining position will alter those effect factors. According to Eq. (14), the effect factors acting on the generalized dynamic flexibilities corresponding to the three frequency segments in y and z directions are represented as Eq. (20). Then, the effect factors for the dynamic flexibilities in the generalized manufacturing space will be predicted. For instance, Fig. 10 describes the change regularities of the effect factors for the dynamic flexibilities of the medium frequency segment in y and z direction with a given value for y coordinate, which is 2.75 dm. As the coordinate (x, z) varies in the generalized manufacturing space, the change regularities of these effect factors caused by the decreased axial and radial dynamic stiffness of the spindle bearing joints have large differentials in different directions. Since the dynamic flexibilities with a determined direction, the corresponding effect factors also change over the axial displacements. The more the value of the effect factor trends to 0, the smaller the impact acts on the dynamic flexibility at the corresponding location. Thus, after a complete study of the generalized dynamic flexibilities of the whole vertical machining center, the positions

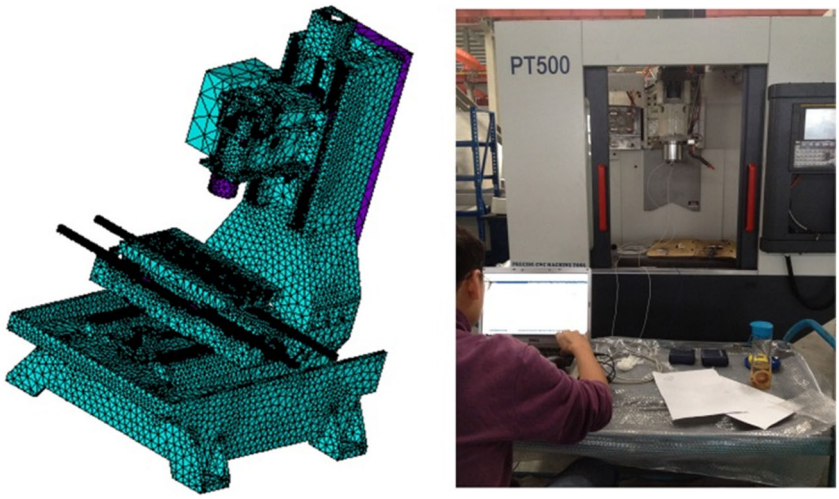

Fig. 7 The whole machine tool FEM and the experiment

Table 4 The factors and their levels

Level	Displacement/m			Stiffness/ (10^8N/m)	
	x	y	z	k_a	k_r
1	0.02	0.02	0.02	0.53	3.45
2	0.1	0.1375	0.1	0.82	4.49
3	0.2	0.275	0.2	1.10	5.52
4	0.3	0.4125	0.3	1.34	6.32
5	0.4	0.55	0.4	1.58	7.11

with a smaller effect factor should be taken into firstly when draft the machining path planning to avoid the unfavorable changes of the dynamic flexibilities at the spindle nose.

5 Conclusions

In this study, a generalized dynamic response model containing the effects of the spatial poses and joint dynamic parameters was developed to analyze the dynamic characteristics of the whole machine tool in the manufacturing space. The RSM theory and the orthogonal experiment design theory are combined to build this generalized dynamic response model, in which the dynamic flexibilities at the spindle nose in different directions and frequency segments are determined to be the objectives representing the whole machine tool dynamic characteristics. The axial and angular displacements and the dynamic stiffness of the spindle bearing joints are determined to be the design variables. The obtained dynamic flexibilities are derived from the simulations arranged by the orthogonal experiment design with the validated whole machine tool FEM, and they are selected as the inputs of the generalized dynamic

Table 5 The orthogonal experiment table

Order	x	y	z	k_a	k_r
1	1	1	1	1	1
2	1	2	2	2	2
3	1	3	3	3	3
4	1	4	4	4	4
5	1	5	5	5	5
6	2	1	2	3	4
7	2	2	3	4	5
8	2	3	4	5	1
9	2	4	5	1	2
10	2	5	1	2	3
11	3	1	3	5	2
12	3	2	4	1	3
13	3	3	5	2	4
14	3	4	1	3	5
15	3	5	2	4	1
16	4	1	4	2	5
17	4	2	5	3	1
18	4	3	1	4	2
19	4	4	2	5	3
20	4	5	3	1	4
21	5	1	5	4	3
22	5	2	1	5	4
23	5	3	2	1	5
24	5	4	3	2	1
25	5	5	4	3	2

Table 6 The validity standards

	$w_{dy\omega l}$	$w_{dy\omega m}$	$w_{dy\omega h}$	$w_{dz\omega l}$	$w_{dz\omega m}$	$w_{dz\omega h}$
RMSE	0.0046	0.0093	0.0082	0.0054	0.0126	0.0046
R^2	0.9821	0.9611	0.9651	0.9816	0.9371	0.9842

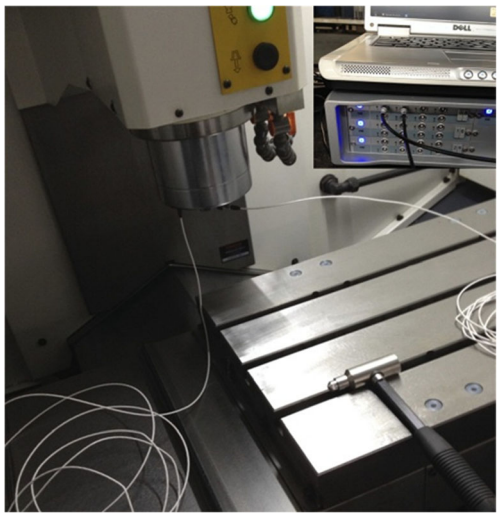

Fig. 8 The dynamic experiments

Table 7 The orthogonal experiment arrangement

Order	Factors		
	x Level	y	z
1	1 (0.15 m)	1 (0.21 m)	1 (0.15 m)
2	1 (0.15 m)	2 (0.34 m)	2 (0.25 m)
3	1 (0.15 m)	3 (0.48 m)	3 (0.35 m)
4	2 (0.25 m)	1 (0.21 m)	2 (0.25 m)
5	2 (0.25 m)	2 (0.34 m)	3 (0.35 m)
6	2 (0.25 m)	3 (0.48 m)	1 (0.15 m)
7	3 (0.35 m)	1 (0.21 m)	3 (0.35 m)
8	3 (0.35 m)	2 (0.34 m)	1 (0.15 m)
9	3 (0.35 m)	3 (0.48 m)	2 (0.25 m)

response model to establish the quadratic polynomial to interpret the relationships between the objectives and the design variables, and the accuracy of the established generalized dynamic response model is validated by the dynamic experiments. Then, the dynamic characteristics of the whole machine tool in the generalized manufacturing space can be predicted. Based on this established model, the proposed algorithm can calculate the effect factors acting on the dynamic flexibilities at the spindle nose, which are brought about by the decreased dynamic stiffness.

$$\begin{cases} E_{ky\omega_l} = \dfrac{|0.1646x-0.1126y+1.1169z-7.0485-0.0533x-0.2085y-0.0808z+0.8933-0.5642|}{|w_{dy\omega_l}|} \\ E_{ky\omega_m} = \dfrac{|0.9244x+0.0895y-2.5617z-14.1139-0.511x-0.1182y-0.0349z+1.2642+1.7436|}{|w_{dy\omega_m}|} \\ E_{ky\omega_h} = \dfrac{|-1.6250x-0.0253y-2.9648z-6.9702-0.2999x-0.0342y+0.0019z+0.4752+1.1052|}{|w_{dy\omega_h}|} \\ E_{kz\omega_l} = \dfrac{|+0.7938x+0.1119y-2.5803z-6.6338-0.4084x-0.0342y+0.0076z+0.4556+1.5403|}{|w_{dz\omega_l}|} \\ E_{kz\omega_m} = \dfrac{|0.138x+0.0651y-0.4805z+0.4017-0.1040x+0.0386y+0.0318z+0.0194+0.3164|}{|w_{dz\omega_m}|} \\ E_{kz\omega_h} = \dfrac{|-3.0284x-0.0247y-4.3054z-5.5896-0.4094x-0.0331y+0.0740z+0.5897+1.1813|}{|w_{dz\omega_h}|} \end{cases} \quad (20)$$

The theory and methods aforementioned have been applied in a three-axis vertical machining center, whose FEM based on the identified joints dynamic parameters are validated. Adopting this FEM to conduct the simulations arranged by the orthogonal experiment design, with the simulated results, a quadratic polynomial containing five variables has been established to represent the generalized dynamic response model. These variables include the axial displacements of the x, y, and z directions and the axial and radial dynamic stiffness of the spindle bearing joints. The calculated RMSE

Table 8 The validity standards

Position		Dynamic flexibility/(10^{-8} m/N)								
		Predicted			Experimental			Errors/(%)		
		Low	Medium	High	Low	Medium	High	Low	Medium	High
1	y	4.96	2.17	1.21	4.92	2.13	1.17	0.78	1.91	3.33
	z	0.58	3.05	7.29	0.60	2.97	7.32	3.69	0.24	0.41
2	y	5.15	2.93	2.10	5.12	2.87	2.02	0.73	2.61	3.62
	z	0.11	3.05	6.40	0.13	3.04	6.48	1.54	0.18	1.27
3	y	5.30	4.43	3.68	5.26	4.32	3.57	0.65	2.46	2.95
	z	0.87	3.20	4.41	0.86	3.19	4.54	1.17	0.12	2.93
4	y	4.41	4.03	3.26	4.38	3.92	3.14	0.61	2.99	3.64
	z	1.07	2.83	4.04	1.14	2.83	4.18	6.14	0	3.34
5	y	4.65	6.61	6.00	4.63	6.46	5.85	0.56	2.34	2.54
	z	2.98	2.75	0.40	2.86	2.75	0.49	4.01	0	3.21
6	y	2.65	1.04	1.53	2.72	1.01	1.51	2.56	2.84	1.22
	z	2.96	2.90	8.12	2.96	2.91	8.15	0.22	0.29	0.41
7	y	3.20	9.62	9.01	3.18	9.43	8.83	0.49	2.06	2.15
	z	5.87	2.29	4.46	5.72	2.30	4.31	2.65	0.34	3.48
8	y	1.63	0.62	0.05	1.71	0.61	0.051	4.54	2.75	1.96
	z	1.39	2.61	5.34	1.42	2.62	5.43	2.25	0.54	1.67
9	y	1.76	3.19	2.67	1.84	3.14	2.61	4.40	1.53	2.19
	z	0.77	2.55	1.79	0.82	2.57	1.84	6.10	0.62	2.72

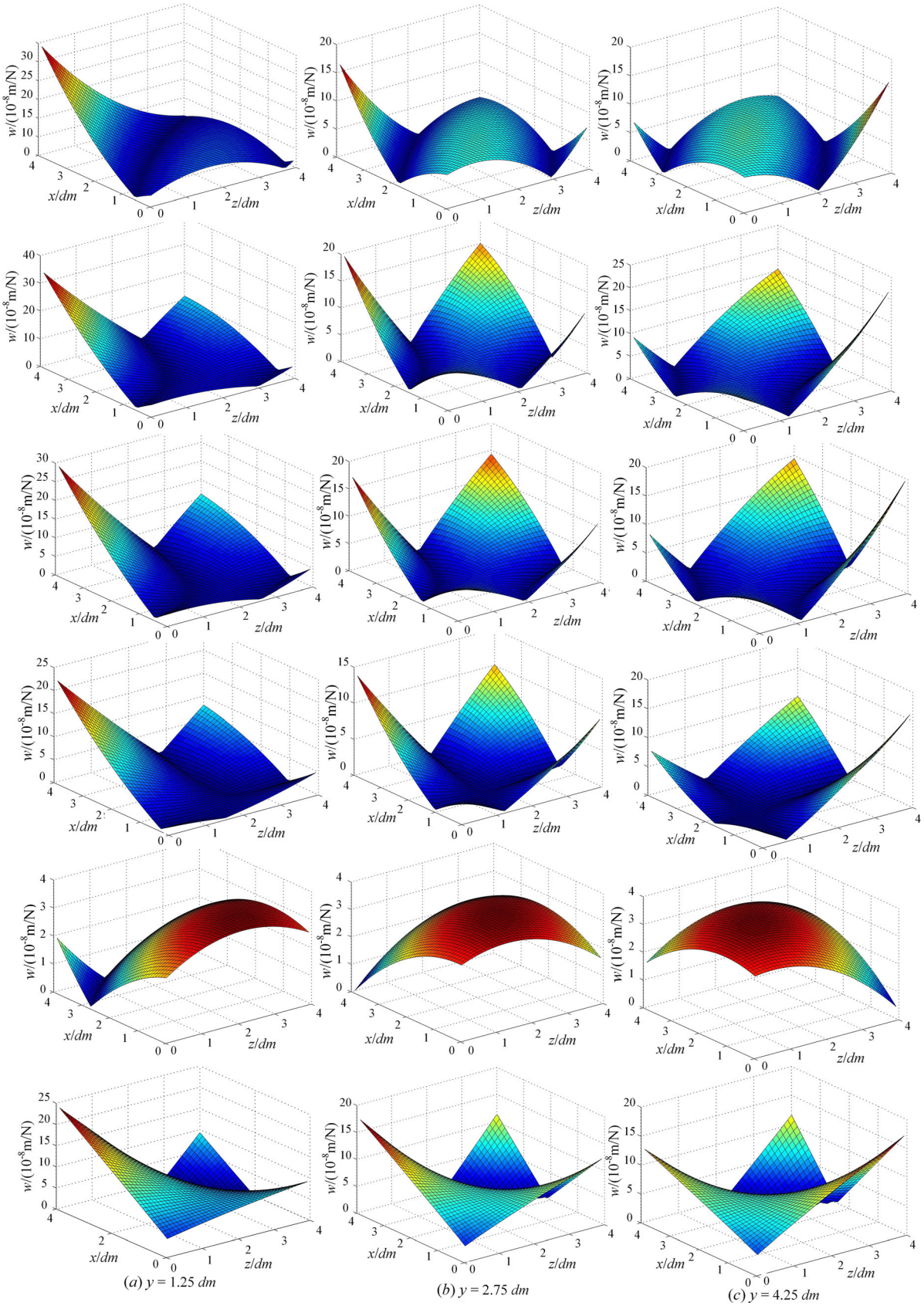

Fig. 9 The generalized dynamic flexibilities at three different locations along the *y* direction

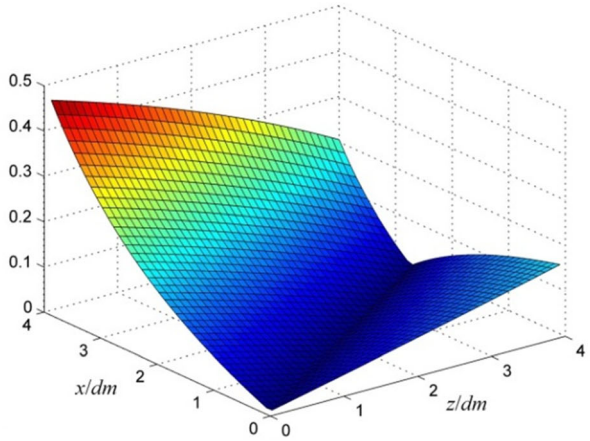

(a) the medium frequency segment (200-400) of the y direction

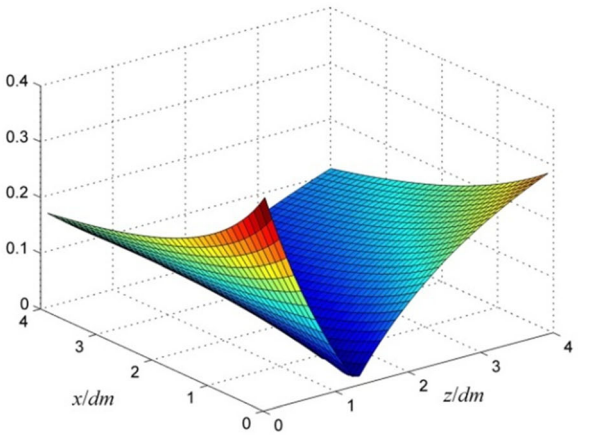

(b) the medium frequency segment (200-400) of the *z* direction

Fig. 10 Effect factors for a *y* axial displacement 2.75 dm

and R^2 validate the good fitting degree of this model. Further nine dynamic experiments were also conducted to verify its feasibility. Three specific *y* coordinates, together with the variable *x* and *z* coordinates are selected as an instance to describe the changes of the dynamic flexibilities of each direction and frequency segment. It is observed that the changing positions have different impacts on the generalized dynamic flexibilities, for they belong to different directions and frequency segments. Also, the calculated effect factors for the *y* and *z* directional dynamic flexibilities of the medium frequencies at a designed *y* coordinate are taken as the examples to illustrate that the decreased axial and radial dynamic stiffness acts differently on the dynamic flexibilities for the changing machining positions.

All the observed results show the changes of the whole machine tool dynamic characteristics in the manufacturing space. And the proposed generalized dynamic response model and joint effect factors calculating algorithm can be integrated to research how the machining poses and joint dynamic parameters influence the dynamic flexibilities at the spindle nose in different directions and frequency segments effectively. They provide a new analytic approach and technique support for the dynamic design of the whole machine tool and lay a basis on the optimal planning of the processing pose and path. For further study, after the connect relationships between the spindle system and the clamping holder-tool system are deeply researched, the model and methods proposed in this paper can be utilized to obtain the tool point dynamic information in the machining space, which will offer more accurate predictions of the machine tool dynamics.

Acknowledgements This research is sponsored by National Science and Technology Support Project and Science and Technology Support Project of Sichuan Province. (NO.2015BAF27B01 & NO.2014GZ0125).

References

1. Lee SW, Mayor R, Ni J (2005) Dynamic analysis of a mesoscale machine tool. J Manuf Sci Eng 128(1):194–203
2. Liang YC, Chen WQ, Bai QS, Sun YZ, Chen GD, Zhang Q, Sun Y (2013) Design and dynamic optimization of an ultraprecision diamond flycutting machine tool for large KDP crystal machining. Int J Adv Manuf Technol 69:237–244
3. Wang YL, Wu XF, Feng HT(2012) Static and dynamic characteristics optimization for a whole large-sized thread grinder based on joint surface. Journal of Vibration and Shock 31(20): 147–152
4. He SP, Mao XY, Liu XQ, Luo BO, Li B, Peng FY (2016) A new approach based on modal mass distribution matrix to identify weak components of machine tool structure. Int J Adv Manuf Technol 83(1):193–203
5. Park SS, Chae J (2008) Joint identification of modular tools using a novel receptance coupling method. Int J Adv Manuf Technol 35: 1251–1262
6. Hung JP, Lai YL, Luo TZ (2013) Analysis of the machining stability of a milling machine considering the effect of machine frame structure and spindle bearings: experimental and finite element approaches. Int J Adv Manuf Technol 68:2393–2405
7. Kolar P, Sulitka M, Janota M (2011) Simulation of dynamic properties of a spindle and tools ystem coupled with a machine tool frame. Int J Adv Manuf Technol 54(1):11–20
8. Altintas Y, Brecher C, Weck M, Witt S (2005) Virtual machine tool. CIRP Keynote Paper 54(2):115–138
9. Zaeh M, Siedl D (2007) A new method for simulation of machining performance by integrating finite element and multi-body simulation for machine tools. CIRP Annals- Manufacturing Technology 56(1):383–386
10. Yang QD, Liu GQ, Wang KH (2008) Dynamics analysis of special structure of milling-head machine tool. Chinese Journal of Mechanical Engineering 21(6):103–107
11. Zhang GH, Ehmann KF (2015) Dynamic design methodology of high speed micro-spindles for micro/meso-scale machine tools. Int J Adv Manuf Technol 76(1):229–246
12. Wu J, Wang JS, Wang LP, Li T, You Z (2009) Study on the stiffness of a 5-DOF hybrid machine tool with actuation redundancy. Mech Mach Theory 44(2):289–305
13. Zaghbani I, Songmene V (2009) Estimation of machine-tool dynamic parameters during machining operation through operational modal analysis. Int J Mach Tools Manuf 49(12–13):947–957
14. Liu HT, Zhao WH (2010) Dynamic characteristic analysis for machine tools based on concept of generalized manufacturing space. Journal of Mechanical Engineering 46(21):54–60

15. Sun MN, Yin GF, Hu T, Hu XB (2013) Method of dynamic stiffness participation factors identification of machine tool joints based on the generalized dynamic information model. Journal of mechanical engineering 49(11):61–69
16. Li TJ, Ding XH, Cheng K (2015) Machine tool dynamics based on spatial statistics. Journal of mechanical engineering 51(21): 87–94
17. Huang H, Zhang SY, Liu XJ, He ZX (2015) Research on cutting stability of generalized manufacturing space based on response surface mode. Journal of zhejiang university (engineering science) 49(7):1215–1223
18. Law M, Phani AS, Altintas Y (2013a) Position-dependent multibody dynamic modeling of machine tools based on improved reduced order models. Journal of Manufacturing Science & Engineering 135(2):2186–2199
19. Ding WZ, Huang XD, Wang ML, Zhu SQ (2013) An approach to evaluate the effects of nonlinear traveling joints on dynamic behavior of large machine tools. Int J Adv Manuf Technol 68(9):2025–2232
20. Chen K (2009) Machine tool design. Springer, London
21. Yan R, Chen W, Peng FY (2012) Closed-loop stiffness modeling and stiffness index analysis for multi-axis machining system. Journal of Mechanical Engineering 48(1):177–184
22. Wu WJ, Liu Q (2011) Dynamics analysis of aparallel mill-turn tool spindle head driven by dual-linear motors using extended transfer matrix method. Chinese Journal of Mechanical Engineering 24(5): 859–869
23. Cao HG, Li B, He ZJ (2012) Chatter stability of milling with speed-varying of spindles. International Journal of Machine Tool & Manufacture 52(1):50–58
24. Zhang J, Schmitz T, Zhao WH, Lu BH (2013) Receptance coupling for tool point dynamics prediction on machine tools. Chinese Journal of Mechanical Engineering 24(3):340–345
25. Chen X, Zhao J, Zhang W (2016) Process optimization and typical application based on geometrical analysis and response surface method for high-speed five-axis ball-end milling operation. Int J Adv Manuf Technol. doi:10.1007/s00170-016-9143-x
26. Liu S (2015) Multi-objective optimization design method for the machine tool's structural parts based on computer-aided engineering. Int J Adv Manuf Technol 78(5):1053–1065
27. Mi L, Yin GF, Sun MN (2012) Effects of preloads on joints on dynamic stiffness of a whole machine tool structure. J Mech Sci Technol 26:495–508
28. Jiang SY, Zhu SL (2010) Dynamic characteristic parameters of linear guideway joint with ball screw. Journal of mechanical engineering 4:92–99
29. Deng CY, Yin GF, Fang H, Meng ZYX (2015) Dynamic characteristics optimization for a whole vertical machining center based on the configuration of joint stiffness. Int J Adv Manuf Technol (2015) 76(5):1225–1242
30. Liao BY, Zhou XM, Yin ZH (2004) Modern mechanical dynamics and its application: modeling, analysis, simulation, modification, control, optimization. Beijing.
31. Zhang XL (2002) The dynamic characteristics of machine joint surface and its application. Beijing.
32. Huang YM (1985) The research of contact rigidity of machine tools slide ways and its influence factors. Journal of Xi'an University of Technology 3:16–25
33. Law M, Altintas Y, Srikanth A (2013b) Rapid evaluation and optimization of machine tools with position dependent stability. Int J Mach Tools Manuf 68(3):81–90